2010 IEEE International Conference on Robotics and Automation
Anchorage Convention District
May 3-8, 2010, Anchorage, Alaska, USA

Eulerian ZMP Resolution based Bipedal Walking: Discussions on the Intrinsic Angular Momentum Rate Change about Center of Mass

Barkan Ugurlu and Atsuo Kawamura

Abstract— **This paper is aimed at implementing Eulerian ZMP Resolution method to bipedal walking pattern generation. The main strategy in this method is to ensure the dynamic balance by generating feasible ZMP-based CoM trajectories. For this purpose, we employ ZMP equations in spherical coordinates, so that the intrinsic angular momentum rate change about center of mass is included explicitly in a natural way. This fact results in two merits: 1) Undesired torso angle fluctuation and body twists are expected to be more restrainable comparing to other methods in which intrinsic angular momentum information is ignored or zero-referenced. 2) The interference between motions in sagittal and lateral planes can be extracted. In this article, we mainly investigate the first merit and briefly discuss about the second merit. Applying the aforementioned technique, Eulerian ZMP Resolution, we simulated bipedal walking on a 3-D dynamic simulator. Secondarily, we conducted bipedal walking experiments on the actual bipedal robot. In conclusion, we obtained dynamically equilibrated bipedal walking cycles, which satisfactorily verify the efficiency of Eulerian ZMP Resolution technique over conventional methods.**

I. INTRODUCTION

In robotics literature, the research on humanoid robots is considered to be one of the most exciting topics as humanoids are able to interfere within the living human environment. Considering such human environment, people mostly perform walking motion unless some extreme situation occurs. It is well known that a human walks at the average speed of 4∼5 [km/h]. The fastest humanoid walking speed, however, is measured around 3 [km/h][1]. Even though running humanoids can achieve faster motion, there must be enhancements for bipedal walking.

Generally, there are two main approaches for bipedal walking pattern generation: a) Whole-body coordination[2], b) one mass concentrated methods[3][18]. In comparison, whole-body based methods are more accurate but they need relatively larger computation time. Considering our robot's computation system[15], we also follow a one mass concentrated approach.

Being a one mass model based approach, Zero Moment Point[10] (ZMP) is one of the widely used bipedal dynamic balance criteria that arouses from gravity, inertial forces and the Intrinsic Angular Momentum Rate change[1] (IAMR) about Center of Mass (CoM). Since it is comparatively difficult to melt the IAMR expression into ZMP equations, researchers mostly omit this term. However, omitting IAMR causes following problems: a) Actual stepping motion could be unusual. The body and legs perform twisting to cancel the angular momentum about CoM[4][5], b) it may create unnatural torso angle fluctuations[16], c) the motion interference between sagittal and lateral planes vanishes.

In order to prevent these drawbacks, we definitely need to inject necessary amount of torques into CoM. For this purpose, Kajita et. al proposed Resolved Momentum Control[4] (RMC) in which the total momenta and joint motions are related. Though its name evokes a control method, its function is similar to inverse kinematics block as it computes joint motions based on referential translational and angular momentum inputs. In their method, pitch axis angular momentum is deliberately assigned as zero but roll axis angular momentum is included for lateral motion. As another example, Sugihara and Nakamura enhanced boundary relaxation method for 3-D hopping motion planning[3]. In their ZMP-based approach, IAMR terms are firstly ignored then included in the inverse kinematics stage. Dissimilarly to these two methods, we defend that angular momentum information could be directly included during the CoM trajectory generation stage instead of inversing dynamics.

Since our aim is to include angular momentum information during the CoM trajectory generation stage, we should combine IAMR terms with inertial forces and gravity terms in ZMP equations. To achieve this task, Toyota group computed roll axis intrinsic angular momentum term simply by multiplying translational CoM velocity with an inertia element which is obtained by trial and error[5]. Strictly speaking, this is not acceptable as angular momentum is related with inertia, angular CoM velocity and angular CoM acceleration. In addition, Huang et. al expressed ZMP equations with IAMR terms by duplicating equations in 2-D[6]. This is also not acceptable as IAMR expressions in different planes mutually have influence on each other in 3-D.

Yet another problem also appears when summing up all individual links' centroidal IAMR terms without projecting them onto the CoM during ZMP computation[6][7]. Unlike inertial forces terms, IAMR terms are not additive without projecting them all to the CoM. A comprehensive treatise on this issue can be examined in [8].

Considering the aforementioned facts, we composed a method to generate bipedal motions, which may ensure the overall dynamic balance. In our proposed method, we utilized ZMP equations in spherical coordinates, so that IAMR terms are explicitly included in our dynamic equations. Since

B. Ugurlu is with Department of Advanced Robotics, Italian Institute of Technology, Via Morego 30, 16163, Genoa, Italy. A. Kawamura is with Division of Advanced Physics, Department of Electrical and Computer Engineering, Yokohama National University, 79-5 Tokiwadai, Hodogaya-ku, Yokohama 240-8501 Japan. kawamura@ynu.ac.jp

[1]IAMR refers the time derivative of inertia tensor · angular velocity vector multiplication[11]; $\frac{d}{dt}\left\{\tilde{I}\cdot\vec{\omega}\right\}$

978-1-4244-5040-4/10/$26.00 ©2010 IEEE

these terms are included using Euler's equations, we name it Eulerian ZMP Resolution (EZR).

Authors group firstly proposed this method for 2-D case to generate jumping motion on a planar robot[16]. Subsequently, the method is enhanced for 3-D case in order to generate motions for bipedal robots which are assumed to be symmetrical about principle axes[17]. As next step, we improved the method by considering unsymmetrical robot geometry[18]. All in these papers, inertia was updated subsequently as the referential CoM trajectory is generated. In this article, we included inertia update process concurrently throughout CoM trajectory generation phase. Hereby, the offline analysis and online computation of EZR become more efficient.

In the present paper, Eulerian ZMP Resolution is explained in section II. Simulation and experimental results are discussed in section III and finally the paper is concluded in section IV.

II. Eulerian ZMP Resolution: Real-time Bipedal Motion Generation

Our proposed method, EZR, is a trajectory generation technique for motions, which include single support phases such as running and walking. Here, the main idea of trajectory planning is to obtain real-time joint motions that ensure desired ZMP profiles through the single support phase and ensure proper boundary conditions through the double support phase, consecutively.

A. Single Support Phase Trajectory Generation

During the single support phase, we consider the robot as an unsymmetrical body, rotating about a fixed point(foot sole center, FSC) and it is in contact with the floor through a foot which has a rectangular shape. Fig. 1 illustrates such modeling. In this model, CoM position is defined in the spherical coordinate frame by using the parameters CoM length, r, angle θ and angle ϕ. For our convenience, the spherical coordinate frame can be defined as follows[19].

1) Go r units along the +z axis.
2) Rotate the frame through θ about +y axis. (pitch)
3) Rotate the frame through ϕ about +x axis. (roll)

Utilizing such model enables us to combine IAMR terms with inertial forces terms in ZMP equations. Considering

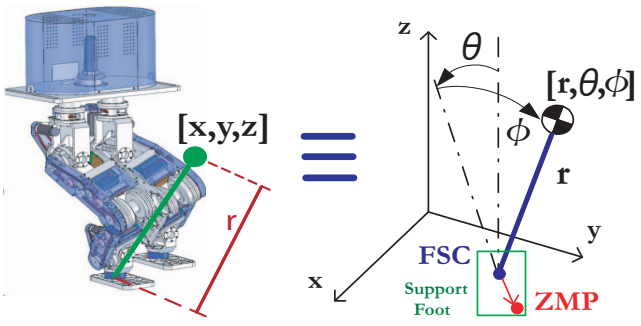

Fig. 1. One Mass Model and Spherical Coordinate System on MARI-3

the z-axis CoM trajectory, z, as constant and determining proper ZMP references, we are able to obtain θ and ϕ angles' trajectories in real-time as we solve ZMP equations iteratively. Performing a conversion from spherical coordinates to Cartesian coordinates gives us x-axis and y-axis CoM trajectories.

Firstly, let us analyze ZMP equations[19]:

$$X_{zmp} = \frac{x(\ddot{z}+g) - z(\ddot{x} - \ddot{X}_{zmp})}{(\ddot{z}+g)} - \frac{\dot{L}_y}{m(\ddot{z}+g)} \tag{1}$$

$$Y_{zmp} = \frac{y(\ddot{z}+g) - z(\ddot{y} - \ddot{Y}_{zmp})}{(\ddot{z}+g)} + \frac{\dot{L}_x}{m(\ddot{z}+g)} \tag{2}$$

In (1) and (2), x, y and z stand for CoM position in Cartesian frame while L_x and L_y symbolize roll axis and pitch axis intrinsic angular momentum about CoM. One dot and two dots represent first and second derivatives with respect to time. Further, m is the total mass and g is the gravitational acceleration. In EZR method, we are going to group ZMP equations into two parts: Inertial Forces Terms and IAMR Terms which are the first and second terms in (1) and (2) respectively. Moreover, ZMP references are constant, so that $\ddot{X}_{zmp}$ and $\ddot{Y}_{zmp}$ becomes zero. Henceforward, we are going to express these terms in the spherical coordinate frame, namely using the parameters r, θ and ϕ.

1) Inertial Forces Terms: In order to express inertial forces terms by using spherical coordinate frame's parameters, we perform necessary coordinate transformation for CoM position. Subsequently, we differentiate position expression two times and obtain CoM acceleration.

$$x = r\sin\theta \tag{3}$$

$$\begin{aligned}\ddot{x} &= \ddot{r}\sin\theta + 2\dot{r}\dot{\theta}\cos\theta + r\ddot{\theta}\cos\theta - r\dot{\theta}^2\sin\theta\end{aligned}$$

$$y = r\cos\theta\sin\phi \tag{4}$$

$$\begin{aligned}\ddot{y} &= \ddot{r}\cos\theta\sin\phi - \dot{r}\dot{\theta}\sin\theta\sin\phi + \dot{r}\dot{\theta}\cos\theta\cos\phi \\ &- \dot{r}\dot{\theta}\sin\theta\sin\phi - r\ddot{\theta}\sin\theta\sin\phi - r\dot{\theta}^2\cos\theta\sin\phi \\ &- r\dot{\theta}\dot{\phi}\sin\theta\cos\phi + \dot{r}\dot{\phi}\cos\theta\cos\phi + r\ddot{\phi}\cos\theta\cos\phi \\ &- r\dot{\theta}\dot{\phi}\sin\theta\cos\phi - r\dot{\phi}^2\cos\theta\sin\phi\end{aligned}$$

$$z = r\cos\theta\cos\phi \tag{5}$$

$$\begin{aligned}\ddot{z} &= \ddot{r}\cos\theta\cos\phi - \dot{r}\dot{\theta}\sin\theta\cos\phi - \dot{r}\dot{\phi}\cos\theta\sin\phi \\ &- \dot{r}\dot{\theta}\sin\theta\cos\phi - r\ddot{\theta}\sin\theta\cos\phi - r\dot{\theta}^2\cos\theta\cos\phi \\ &+ r\dot{\theta}\dot{\phi}\sin\theta\sin\phi - \dot{r}\dot{\phi}\cos\theta\sin\phi - r\ddot{\phi}\cos\theta\sin\phi \\ &+ r\dot{\theta}\dot{\phi}\sin\theta\sin\phi - r\dot{\phi}\end{aligned}$$

2) Intrinsic Angular Momentum Rate Change Terms: Supposing that the friction between the floor and the foot sole is sufficient and there is no foot rotation, we can consider the support phase motion as a rotation of a rigid body about a fixed point as previously stated. For this case, Euler's equations of motion for unsymmetrical bodies might give us insights,

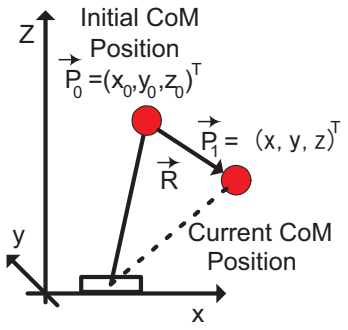

Fig. 2. Inertia varies with respect to CoM Position

$$\begin{aligned}\tau_x = \dot{L}_x &= I_{xx}\dot{\omega}_x - (I_{yy} - I_{zz})\omega_y\omega_z - (\omega_y^2 - \omega_z^2)I_{yz} \\ &\quad -(\omega_x\omega_y + \dot{\omega}_z)I_{xz} + (\omega_x\omega_z - \dot{\omega}_y)I_{xy} \\ \tau_y = \dot{L}_y &= I_{yy}\dot{\omega}_y - (I_{zz} - I_{xx})\omega_z\omega_x - (\omega_z^2 - \omega_x^2)I_{xz} \\ &\quad -(\omega_y\omega_z + \dot{\omega}_x)I_{xy} + (\omega_y\omega_x - \dot{\omega}_z)I_{yz} \\ \tau_z = \dot{L}_z &= I_{zz}\dot{\omega}_z - (I_{xx} - I_{yy})\omega_x\omega_y - (\omega_x^2 - \omega_y^2)I_{xy} \\ &\quad -(\omega_z\omega_x + \dot{\omega}_y)I_{yz} + (\omega_z\omega_y - \dot{\omega}_x)I_{xz}\end{aligned} \tag{6}$$

in which I_{xx}, I_{yy} and I_{zz} are moments of inertia about principle axes, I_{xy}, I_{xz} and I_{yz} are products of inertia, ω_x, ω_y and ω_z are angular velocities about principle axes and τ_x, τ_y and τ_z are rate change of angular momentums (torques) about roll pitch and yaw axes.

In our spherical coordinate frame, second and third steps indicate two rotational actions. Combining two successive these rotations, we may create a rotation matrix. Subsequently, angular velocity vector could be derived out of the rotation matrix as follows by using a tensorial approach[12].[2]

$$\omega_x = -\dot{\phi} \quad , \quad \omega_y = \dot{\theta}\cos\phi \quad , \quad \omega_z = -\dot{\theta}\sin\phi \tag{7}$$

$$\begin{aligned}\dot{\omega}_x &= -\ddot{\phi} \\ \dot{\omega}_y &= \ddot{\theta}\cos\phi - \dot{\theta}\dot{\phi}\sin\phi \\ \dot{\omega}_z &= -\ddot{\theta}\sin\phi - \dot{\theta}\dot{\phi}\cos\phi\end{aligned} \tag{8}$$

As next step, if we combine (7) and (8) in (6), it is possible to obtain IAMR terms as shown below.

$$\begin{aligned}\dot{L}_x &= \ddot{\theta}(I_{xz}\sin\phi - I_{xy}\cos\phi) + 2\dot{\theta}\dot{\phi}(I_{xy}\sin\phi + I_{xz}\cos\phi) \\ &\quad - I_{xz}\ddot{\phi} + \dot{\phi}^2((I_{yy} - I_{zz})\sin\phi\cos\phi - (\cos^2\phi - \sin^2\phi)I_{yz})\end{aligned} \tag{9}$$

$$\begin{aligned}\dot{L}_y &= \ddot{\theta}(I_{yz}\sin\phi + I_{yy}\cos\phi)\dot{\theta}\dot{\phi}\sin\phi(I_{xx} - I_{yy} - I_{zz}) \\ &\quad + \dot{\theta}^2\sin\phi(I_{xy}\cos\phi - I_{xz}\sin\phi) + I_{xy}\ddot{\phi} + I_{xz}\dot{\phi}^2\end{aligned} \tag{10}$$

Having computed the IAMR about CoM, we finally compute inertia tensor as it varies with respect to CoM position.

In Fig. 2, CoM of the robot moves from the initial position $\vec{P}_0$ to some arbitrary position $\vec{P}_1$. In this case, $\vec{R} = \vec{P}_1 - \vec{P}_0$ is the displacement vector. If we know the initial inertia tensor, we can calculate the current inertia tensor as follows.

[2]Please note that, we need one more rotation to demonstrate the most general case since 3 successive rotations are required to define 3-D space. However, as we only concentrate on straight walking without turning/curving, aforementioned definitions fit well to our case.

$$\tilde{I}_{cur} = \tilde{I}_{init} + m\left[\left(\vec{R}\cdot\vec{R}\right)E_3 - \vec{R}\otimes\vec{R}\right] \tag{11}$$

Above, $\tilde{I}_{cur}$, $\tilde{I}_{init}$, E_3, m are the current inertia tensor, initial inertia tensor, 3x3 unit matrix and the total mass, respectively. What is more, $\cdot$ and $\otimes$ symbolize dot product and outer product. In this case, if initial position at $t = 0$ is given (x_0, y_0, z_0), and initial inertia tensor is obtained from CAD data, current inertia elements could be computed as below.

$$\begin{aligned}I_{xx} &= I_{xx0} + m[(r\cos\theta\sin\phi - y_0)^2 + (r\cos\theta\cos\phi - z_0)^2] \\ I_{zz} &= I_{zz0} + m[(r\sin\theta - x_0)^2 + (r\cos\theta\sin\phi - y_0)^2] \\ I_{yy} &= I_{yy0} + m[(r\cos\theta\cos\phi - z_0)^2 + (r\sin\theta - x_0)^2] \\ I_{yz} &= I_{yz0} - m(r\cos\theta\sin\phi - y_0)(r\cos\theta\cos\phi - z_0) \\ I_{xy} &= I_{xy0} - m(r\sin\theta - x_0)(r\cos\theta\sin\phi - y_0) \\ I_{xz} &= I_{xz0} - m(r\sin\theta - x_0)(r\cos\theta\cos\phi - z_0)\end{aligned} \tag{12}$$

In (12), the underscript "0" refers the initial condition when $t = 0$. Please note that, inertia elements in (9) and (10) are calculated as expressed in (12). These equations will be combined in the next subsection.

3) Solving ZMP Equations for θ and ϕ Trajectories: Before solving ZMP equations, we define τ_{zmpx} and τ_{zmpy} which come out from cross multiplications in (1) and (2) to eliminate fractional expressions.

$$\begin{aligned}\tau_{zmpx} &= mX_{zmp}(\ddot{z} + g) = mx(\ddot{z} + g) - mz\ddot{x} - \dot{L}_y \\ \tau_{zmpy} &= mY_{zmp}(\ddot{z} + g) = my(\ddot{z} + g) - mz\ddot{y} + \dot{L}_x\end{aligned} \tag{13}$$

Secondarily, some repeating sub-expressions are defined to ease our calculations.

$$\begin{aligned}\dot{J}_\alpha &= 2mr\dot{r} & \sigma &= mr \\ \mu_6 &= \sin^2\phi & J_\alpha &= mr^2 \\ \mu_4 &= \cos^2\phi & \mu_5 &= \sin^2\theta \\ \mu_1 &= \sin\theta\cos\theta & \mu_3 &= \cos^2\theta \\ \mu_2 &= \sin\phi\cos\phi & \mu_7 &= \sin\theta\sin\phi \\ r &= z\sec\theta\sec\phi & p_4 &= x_0\cos\theta\cos\phi \\ J_{yz} &= I_{yz0} - my_0z_0 & p_6 &= z_0\sin\theta + 2p_4 \\ J_{xy} &= I_{xy0} - mx_0y_0 & J_{xz} &= I_{xz0} - mz_0x_0 \\ p_1 &= y_0\sin\phi + z_0\cos\phi & p_2 &= y_0\cos\phi - z_0\sin\phi \\ I_n &= I_{xx0} - I_{yy0} - I_{zz0} & \dot{r} &= r(\dot{\theta}\tan\theta + \dot{\phi}\tan\phi) \\ J_{yy} &= I_{yy0} + m(z_0^2 + x_0^2) & J_{zz} &= I_{zz0} + m(x_0^2 + y_0^2) \\ p_5 &= y_0\sin\theta + x_0\cos\theta\sin\phi & J_{xx} &= I_{xx0} + m(y_0^2 + z_0^2) \\ p_3 &= x_0\sin\theta + y_0\cos\theta\sin\phi & J_u &= I_{yy0} - I_{zz0} - m(y_0^2 - z_0^2)\end{aligned} \tag{14}$$

Finally, if we insert (3), (4), (5), (9), (10), (12) and (14) into (13), we obtain following equations.

$$
\begin{aligned}
\tau_{zmpx} &= \ddot{\theta}\{\sigma(\cos\phi(p_3 + x_0\sin\theta) + z_0\cos\theta(1+\mu_4)) \\
&\quad - 2J_a\cos\phi - J_{yy}\cos\phi + J_{yz}\sin\phi\} + \ddot{\phi}\{J_{xy} \\
&\quad + \sigma p_5 - 2J_a\mu_1\sin\phi\} + \dot{\theta}^2\{J_{xy}\mu_2 + \sigma p_2\mu_{10} \qquad (15) \\
&\quad - J_{xz}\mu_6\} + \dot{\phi}^2\{J_{xz} + \sigma(p_6 - p_4) - 2J_a\mu_1\cos\phi\} \\
&\quad + \dot{\theta}\dot{\phi}\{4J_a\mu_5\sin\phi + 2mx_0^2\sin\phi - 4\sigma x_0\mu_{10} - I_n\sin\phi\} \\
&\quad - \dot{\theta}\{\dot{J}_a\cos\phi\} - \dot{\phi}\{\dot{J}_a\mu_1\sin\phi\} + mgr\sin\theta \\
\tau_{zmpy} &= \ddot{\theta}\{J_{xy}\cos\phi - J_{xz}\sin\phi + \sigma p_2\sin\theta\} + \ddot{\phi}\{-J_{xx} \\
&\quad + 2\sigma p_1\cos\theta - 2J_a\mu_3\} + \dot{\theta}^2\{J_{yz}\cos 2\phi + J_u\mu_2 \qquad (16) \\
&\quad + \sigma p_2\cos\theta\} + 2\dot{\theta}\dot{\phi}\{2J_a\mu_1 - J_{xy}\sin\phi - J_{xz}\cos\phi \\
&\quad - \sigma p_1\sin\theta - \sigma x_0\cos\theta\} - \dot{\phi}\{\dot{J}_a\mu_3\} + mgr\mu_{11}
\end{aligned}
$$

Equations (15) and (16) describes a pair of coupled second order differential equations. These equations can be solved by using Runge-Kutta method[13] in an iterative fashion when following parameters are designed.

- z-axis CoM trajectory : z
- X_{zmp} and Y_{zmp} input trajectories
- Initial values: $\theta_{[0]}$, $\phi_{[0]}$, $\dot{\theta}_{[0]}$ and $\dot{\phi}_{[0]}$
- Initial CoM Position: x_0, y_0, z_0
- Initial inertia tensor elements: I_{xx0}, I_{yy0}, I_{zz0}, I_{xy0}, I_{xz0}, and I_{yz0} (from CAD data)
- Support Phase Time Interval: (t_{start}, t_{start}+t_{width})
- Swing Leg Parameters: Stride, Foot Height

4) The Interference Between Motions in Sagittal and Lateral Planes: If one can perform a conversion from spherical coordinates to Cartesian coordinates for (9) and (10), it could be seen that both these terms are function of x, $\dot{x}$, $\ddot{x}$, y, $\dot{y}$, $\ddot{y}$, z, $\dot{z}$ and $\ddot{z}$. Thus, we may understand that motions in sagittal and lateral planes are strongly coupled through the intrinsic angular momentum rate change phenomenon. In other words, omitting IAMR terms in ZMP equations makes these motions independent from each other as wrongly comprehended in [9]. Therefore, we strongly believe that if motions in sagittal and lateral planes are to be synchronized, IAMR terms must be considered. This task needs systematic arrangement of these equations in Cartesian frame. We are going to investigate this synchronization task in our next work.

B. Double Support Phase and Swing Leg Trajectories

Double support phase and swing leg trajectories are planned in a similar fashion as proposed in [9]. Double support phase motion is planned using 5^{th} and 6^{th} order polynomials[13] to create a seamless connection between switching single support phases, both in position velocity and acceleration level. Swing leg motion is also designed by considering target forward velocity.

C. CoM-based Inverse Kinematics

In order to calculate joint motions, we proposed an inverse kinematics algorithm that is CoM-based and totally independent from swing leg motion. Our bipedal robot MARI-3's[15] joint frame can be seen in Fig. 4. It has total 13 of

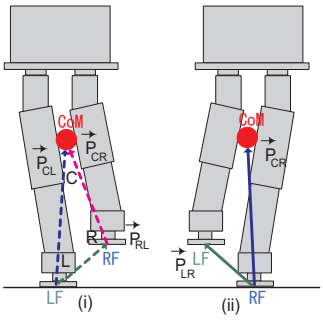

Fig. 3. Single Support Phases

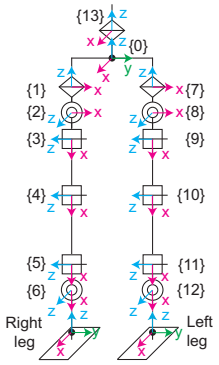

Fig. 4. MARI−3 Frame

DOF(degrees of freedom), 6 DOF in each leg and 1 DOF at the waist. This waist joint has no effect on the CoM position. In each leg, hip joint is 3 DOF (yaw-pitch-roll), knee joint is 1 DOF (pitch) and ankle joint is 2 DOF (pitch-roll). For sake of straight walking on a flat surface, total orientation for both yaw pitch and roll are set to zero. A heuristic relation in this case can be expressed as follows.

$$
\begin{array}{ccc}
q_1 = 0 & q_7 = 0 & (yaw) \\
q_2 + q_6 = 0 & q_8 + q_{12} = 0 & (roll) \\
q_3 + q_4 + q_5 = 0 & q_9 + q_{10} + q_{11} = 0 & (pitch)
\end{array} \qquad (17)
$$

In (17), q symbolizes joint angles. Joint numbers can be found in Fig. 4. Using (17), we are down to 6 variables, namely, $\vec{Q} = [q_2\ q_3\ q_5\ q_8\ q_9\ q_{11}]^T$. As next step, let us suppose that the robot is in the right foot's single support phase as illustrated in Fig. 3-(ii). In this figure, $\vec{P}_{CR}$ and $\vec{P}_{LR}$ are the position vectors from right foot to CoM and left foot, respectively. As aforementioned above, $\vec{P}_{CR}$ is computed from ZMP equations and $\vec{P}_{LR}$ is generated by swing leg motion. Forward kinematics expressions of these position vectors are function of all joints, ($q_1 ... q_{12}$). If we insert (17) into these expressions, they become only the function of $\vec{Q}$ vector defined above. If $\vec{P}$ is assigned as $\vec{P} = [\vec{P}_{CR}\ \vec{P}_{LR}]^T$ we may define a Jacobian matrix between $\vec{P}$ and $\vec{Q}$.

$$
\dot{\vec{P}} = J_R\dot{\vec{Q}} \qquad (18)
$$

Avoiding singularities, (18) could be solved for $\vec{Q}$ by using Newton-Raphson method[13].

However, this method always needs $\vec{P}_{CR}$ and $\vec{P}_{LR}$ vectors, which are defined with respect to right foot. When the robot is in the left foot's single support phase, we would have $\vec{P}_{CL}$ and $\vec{P}_{RL}$ which are the CoM and right foot position vectors with respect to the left foot as seen in Fig. 3-(i). In order to calculate $\vec{P}_{CR}$ and $\vec{P}_{LR}$ by using $\vec{P}_{CL}$ and $\vec{P}_{RL}$ we may use vector subtractions, indicated in $L\hat{C}R$ triangle, Fig. 3-(i).

$$
\begin{aligned}
\vec{P}_{CR} &= \vec{P}_{CL} - \vec{P}_{RL} \\
\vec{P}_{LR} &= -\vec{P}_{RL}
\end{aligned} \qquad (19)
$$

Having obtained $\vec{P}_{CR}$ and $\vec{P}_{LR}$ out of $\vec{P}_{CL}$ and $\vec{P}_{RL}$, we can use (18) and compute all joint motions. Please note that,

the above transformation can only be used when orientation references are substituted to zero as we performed in (17). For non-zero orientation references, refer to [20].

When the robot is in the double support phase, $\vec{P}_{LR}$ is fixed and remains constant. In that case, $\vec{P}_{CR}$ is derived by using polynomials as we mentioned above. Thus, we can compute all joint motions simply by using (18).

III. Simulation and Experimental Results

To be able to validate our proposed method, we firstly simulated bipedal walking motion on a 3-D dynamic simulator[14] using the realistic model of our bipedal robot. Furthermore, we conducted bipedal walking experiments on MARI-3[15].

A. Simulation Results

In this simulation, single and double support phases are planned as 0.4 [s] and 0.2 [s]. Referential ZMP inputs are not time varying and they are substituted as 0.045 [m] and $\pm$ 0.02 [m] for x-axis and y-axis, respectively. Results may be observed from Fig. 5 to Fig. 10.

In Fig. 5 Ground Reaction Force variations for right foot(red) and left foot(blue) are shown. Switching between right and left feet can be observed in this figure.

Torso angle variation for roll and pitch axes are plotted in Fig. 6. In this figure, solid red and solid blue lines are illustrating torso angle variations for roll axis and pitch axis while IAMR terms are included. In contrast, dot green and dot magenta lines indicate torso angle variations while IAMR terms are zero-referenced. Comparing these two cases, we can observe that torso angle fluctuation can be suppressed when IAMR terms are included.

CoM trajectories for x-axis and y-axis can be seen in Fig. 7 and Fig. 8. In these figures, solid red and dot green lines are symbolizing CoM trajectories' referential and response values with respect to the right foot. In the same manner, solid blue and dot magenta lines are symbolizing CoM trajectories' referential and response values with respect to the left foot. Based on these figures, we can say that trajectory responses follow their references well. In addition, transition between left/right single support phases and double support phases are tied successfully.

x-axis and y-axis ZMP responses of right foot are illustrated in Fig. 9 and Fig. 10. In these figures, yellow areas symbolize single support phases. As it may be observed, ZMP responses are always within the support polygon boundaries. Additionally, we do not plot right foot's ZMP responses during left foot single support phases.

B. Experimental Results

Having obtained successful walking simulations, we conducted bipedal walking experiments on the actual robot MARI-3. Walking parameters are determined in the same fashion as determined in the simulation. Results can be seen from Fig. 11 to Fig. 16.

Right foot's ZMP responses are plotted in Fig. 11 and Fig. 12. Solid red, dot blue and dot green lines are indicating ZMP response and support polygon boundaries, respectively. As ZMP responses both for x-axis and y-axis are always within the support polygon, we obtained dynamically equilibrated bipedal walking cycles. Furthermore, light orange areas symbolize the right leg swinging periods. Since the right foot has no contact with the floor while swinging, we do not plot its ZMP. Please note that, left foot's ZMP response is identical to right foot's ZMP response.

x-axis and y-axis CoM trajectories' response values may be observed in Fig. 13 and Fig. 14. In these figures, blue and cyan lines are pointing out CoM trajectories with respect to right foot and left foot, respectively. These plots may indicate that transitions between left/right foot single support phases and double support phases are connected seamlessly.

Finally, roll and pitch axis torso angle variations are shown in Fig. 15 and Fig. 16. Similar to the comparison that is performed in the simulation, we also measured torso angle variations both for with and without IAMR terms included. When we force IAMR about CoM to be zero, roll axis torso angle varies between $\pm$ 6 degrees and pitch axis torso angle varies between $\pm$ 10 degrees as cyan lines indicate. Furthermore, MARI-3 suffered undesired stepping motions between 2.8 seconds to 4 seconds, indicated with gray areas. In contrast to this situation, torso angle variations are suppressed well if IAMR terms are included. This case is plotted with blue lines in these figures. Moreover, there was no undesired stepping motion. Based on this comparison, one can argue that the IAMR is a very important index for feasible bipedal motion planning.

IV. Conclusion

To sum up, we proposed a systematic way of generating ZMP-based CoM trajectories for bipedal motion generation without ignoring or referencing intrinsic angular momentum information. Unlike other methods in which IAMR around CoM is forced to be zero, certain amount of undesired torso angle fluctuation is reduced. This certainly enables us to obtain more feasible bipedal motion planning.

Moreover, inertia update process is combined with our dynamic ZMP equations. Hence, the offline analysis and real-time computation of EZR-based bipedal trajectory generation become more efficient.

Nonetheless, we validate Eulerian ZMP Resolution by conducting bipedal walking simulations and experiments. Since we already employed EZR for running, jogging and jumping trajectories in our previous works[18][17][16], we may say that our method is suitable for most of the bipedal motion generation. Furthermore, we believe that Eulerian way of resolution could be applied to other methods which represent robot dynamics by considering the rate change of angular momentum vector.

Having obtained successful bipedal walking simulation and experimental results, our next work is to employ Eulerian ZMP Resolution to succeed faster motions on the bipedal robot MARI-3. Additionally, we are going to discuss about the synchronization of motions in sagittal and lateral planes in a systematic manner.

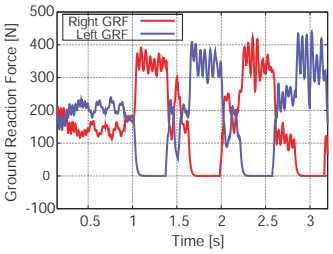

Fig. 5. GRF Response, Simulation

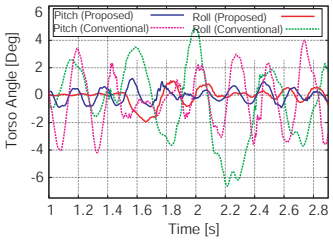

Fig. 6. Torso Angles, Simulation

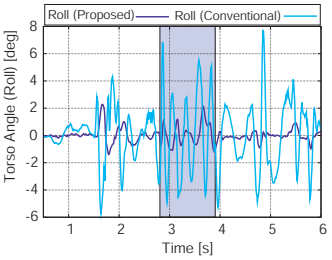

Fig. 15. Roll Angle, Experiment

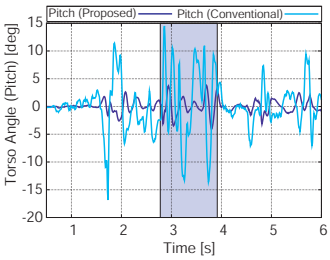

Fig. 16. Pitch Angle, Experiment

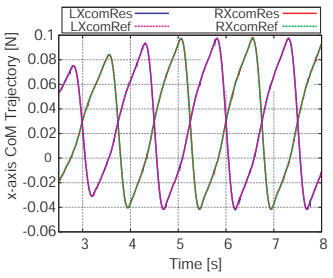

Fig. 7. x−axis CoM, Simulation

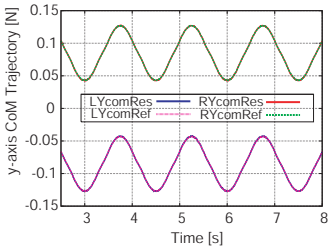

Fig. 8. y−axis CoM, Simulation

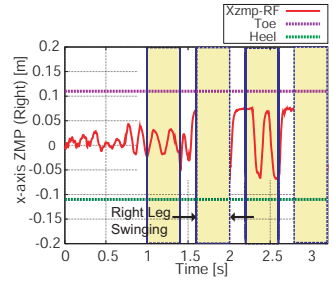

Fig. 9. x−axis ZMP, Simulation

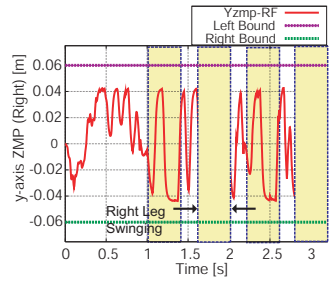

Fig. 10. y−axis ZMP, Simulation

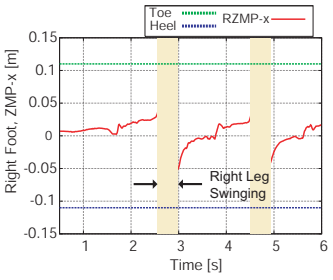

Fig. 11. x−axis ZMP, Experiment

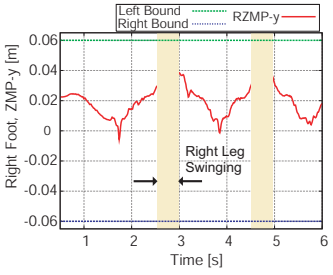

Fig. 12. y−axis ZMP, Experiment

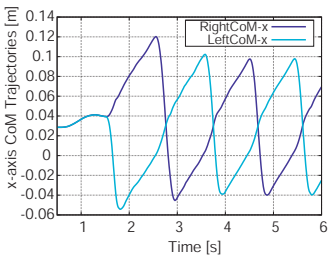

Fig. 13. x−axis CoM, Experiment

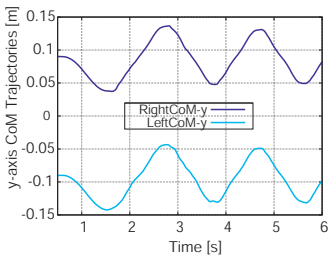

Fig. 14. y−axis CoM, Experiment

REFERENCES

[1] T. Takenaka, T. Matsumoto, and T. Yoshiike, "Real time motion generation and control for biped robot-1^{st} report: Walking gait pattern generation," in *Proc. IEEE Conf. Intl. Robots and Systems*, St. Louis, US, 2009, pp. 1084-1091.

[2] Y. Fujimoto, S. Obata and A. Kawamura, "Robust bipedal walking with active interaction control between foot and ground," in *Proc. IEEE Conf. Rob. and Auto.*, Belgium, 1998, pp. 2030-2035.

[3] T. Sugihara, and Y. Nakamura, "Enhancement of boundary condition relaxation method for 3D hopping motion planning of biped robots," in *Proc. IEEE Conf. Int. Robots and Systems*, US, 2007, pp. 444-449.

[4] S. Kajita, K. Kaneko, M. Morisawa, S. Nakaoka, and H. Hirukawa, "ZMP-based biped running enhanced by toe springs," in *Proc. IEEE Conf. Rob. and Auto.*, Italy, 2007, pp. 3963-3969.

[5] R. Tajima, D. Honda, and K. Suga, "Fast running experiments involving a humanoid robot," in *Proc. IEEE Conf. Rob. and Auto.*, Japan, 2009, pp. 1571-1576.

[6] Q. Huang, K. Yokoi, S. Kajita, K. Kaneko, H. Arai, N. Koyachi, and K. Tanie "Planning walking patterns for a biped robot," in *Trans. on Rob. and Auto.*, vol. 17, no. 3, 2001, pp. 280-289.

[7] A. Hofmann, M. Popovic, and H. Herr, "Exploiting angular momentum to enhance bipedal center-of-mass control," in *Proc. IEEE Conf. Rob. and Auto.*, Japan, 2009, pp. 4423-4429.

[8] D. E. Orin, and A. Goswami, "Centroidal Momentum Matrix of a humanoid robot: Structure and properties," in *Proc. IEEE Conf. Intl. Robots and Systems*, France, 2008, pp. 653-659

[9] C. Zhu, Y. Tomizawa, and A. Kawamura "Bipedal walking pattern design based on synchronization of the motions in sagittal and lateral planes," in *Proc. IEEE Conf. Intl. Robots and Systems*, Canada, 2005, pp. 4101-4107.

[10] M. Vukobratovic, and B. Borovac, "Zero-Moment Point - Thirty Five Years of its Life," in *Int. Journal of Humanoid Rob.*, Vol 1, No. 1, 2004, pp. 157-173.

[11] R.Featherstone, *Robot Dynamics Algorithms*,Kluwer Acad. Pub.,1987.

[12] C. A. Balafoutis, and R. V. Patel, *Dynamic Analysis of Robot Manipulators: A Cartesian Tensor Approach*, Kluwer Acad. Pub., 1991.

[13] W. H. Press, S. A. Teukolsky, W. T. Vetterling, and B. P. Flannery *Numerical Recipes in C: The Art of Scientific Computing* 2^{nd} *Edition*, Cambridge University Press, 1992.

[14] Y. Fujimoto, and A. Kawamura "Simulation of an autonomous biped walking robot including environmental force interaction," in *IEEE Rob. and Auto. Magazine*, vol. 5, no. 2, 1998, pp. 33-42.

[15] A. Kawamura, and C. Zhu "The development of biped robot MARI-3 for fast walking and running," in *Proc. IEEE Conf. Intl. Robots and Systems*, China, 2006, pp. 599-604.

[16] B. Ugurlu, and A. Kawamura, "Real-time jumping trajectory generation for a one legged jumping robot," in *Proc.Int. Conf. on Industrial Electronics and Control*, US, 2008, pp. 1668-1673.

[17] B. Ugurlu, and A. Kawamura, "Eulerian ZMP resolution: Real-time jogging and jumping trajectory planning for bipedal robots," in *Proc. IEEE Conf. Adv. Intl. Mechatronics*, Singapore, 2009, pp. 150-155.

[18] B. Ugurlu, and A. Kawamura, "Real-time running and jumping pattern generation for bipedal robots based on ZMP and Euler's equations," in *Proc. IEEE Conf. Intl. Robots and Systems*, US, 2009, pp. 1100-1105.

[19] B. Ugurlu, *Bipedal Motion Planning based on Composite Rigid Body Angular Momentum Resolution*, PhD Dissertation, Yokohama National University, Yokohama, Japan 2010.

[20] F. Ali, B. Ugurlu, and A. Kawamura, "Center of mass based inverse kinematics algorithm for bipedal robot motion on inclined surfaces," in *Proc. IEEE Works. Adv. Motion Control*, Japan, 2010, to be presented.